BOND GRAPH BASED MODELLING AND SIMULATION OF FLEXIBLE ROBOTIC MANIPULATORS

Vjekoslav Damic
University of Dubrovnik
Department of Mechanical Engineering
Cira Carica 4, 20000 Dubrovnik, Croatia
vdamic@unidu.hr

Majda Cohodar
University of Sarajevo
Faculty of Mechanical Engineering
Vilsonovo setaliste 9, Sarajevo, B&H
cohodar@mef.unsa.ba

KEYWORDS

Bond Graphs, Flexible manipulator, Finite-element beams, Co-rotational formulation, Differential-algebraic equations.

ABSTRACT

Modern lightweight robotic systems require a systematic, multidisciplinary approach to design. Bond graphs provide a general paradigm that can be used in design of such complex systems.

Modelling of slender manipulator links that typically undergo large translational and rotational motion is not simple. There are several approaches that are developed. In this paper slender robotic links are modelled as a collection of finite element beams based on co-rotational formulation.

The model of a complete robotic system is developed using multi-level bond graph models. The resulting mathematical model is generated in the form of a system of differential-algebraic equations (DAEs). One advantage of using bond graphs is that the model formulation is based on velocities (unlike other methods that typically use position formulation) and that leads to index 2 semi-explicit DAEs, which can be readily solved with available techniques.

BondSim, an integrated object-oriented modelling and simulation environment, is used. The method is applied to two flexible multi-link problems and simulation results show that developed models provide excellent numerical performances. The proposed method can be successfully used for modelling other mechatronics systems as well.

1. INTRODUCTION

The demand for better productivity leads to the application of high-speed and lightweight robot manipulators. As a consequence, rigid-body assumptions are not valid and hence it is necessary to deal with flexible manipulators under feedback control.

Investigation of flexible multibody systems was the subject of extensive research for many years. It was shown that modelling flexible systems that undergo large translation and/or rotational displacement is not a simple problem. Several approaches are developed to deal with such problems (Rankin and Brogan 1986, Avelo et al 1991, Crisfield and Moita 1996, Shabana 1998).

Application of bond graph technique on multibody systems was the subject of many investigations. In (Karnopp 1997) the emphasis is on understanding of multibody dynamics using the bond graph representation. In (Favre and Scavarda 1998) a procedure for building the bond graph representation of multibody systems with kinematics loops has been proposed, while in (Damic and Montgomery 2003) bond graphs are efficiently used for modelling rigid multibody systems. In (Margolis and D. Karnopp 1979) a linear bond graph approach based on normal mode decomposition is described.

This paper explores the possibility of using the bond graph technique in investigation of dynamic behaviour of lightweight manipulators with long links that operate at high speeds. The robot links are modelled as flexible 3D beams. Between several approaches, which have been applied to flexible multibody systems undergoing large translation and/or rotation motions, the co-rotational approach (Rankin and Brogan 1986, Nour-Omid and Rankin 1991, Pacoste and Eriksson 1997, Damic and Cohodar 2005, Damic 2006) has been used herein because it offers several advantages to the modeller:

- Nonlinear framework,
- Separation of rigid-body motions and element deformations,
- Description of deformation using well known constitutive relations,
- Interconnecting component models of flexible bodies in a similar way as when building rigid-body models.

The bond graph approach naturally leads to velocity formulation of mathematical models of multibody systems. The model is generated in the form of semi-explicit systems of differential algebraic equations of index 2 that can be readily solved using available techniques. The component model approach is most effectively implemented using object-oriented techniques. The BondSim application (Damic and Montgomery 2003) is specifically developed to facilitate this modelling approach. The models are developed in the form of trees of component models. At every level of decomposition, the corresponding word models are described by separate bond graph

Proceedings 20th European Conference on Modelling and Simulation
Wolfgang Borutzky, Alessandra Orsoni, Richard Zobel © ECMS, 2006
ISBN 0-9553018-0-7 / ISBN 0-9553018-1-5 (CD)

component documents. The leaves of a model tree are familiar bond graph elementary components.

Numerical examples presented in the paper show that the developed method enables relatively simple changing of rigid-body models to partially or completely flexible-body models. In addition, the complete control loop is also closed around the manipulator. Thus using bond graphs, it is possible to study dynamic behaviour of complete robot systems.

2. MODEL OF FLEXIBLE LINK

2.1. Co-rotational formulation

Flexible links of a robot system are assumed to be long and slender, and they can be represented by beam finite elements. The element initially is straight and deforms under the action of forces.

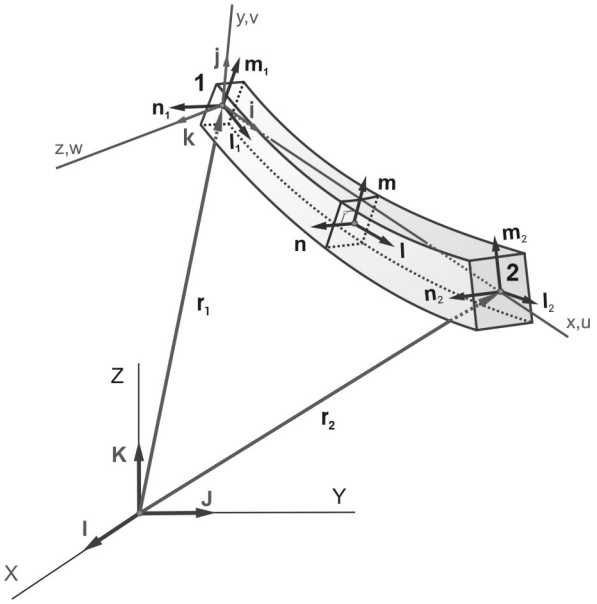

Figure 1: Coordinate frames of co-rotation formulation

Several coordinate frames are defined (Fig.1):

1. *Global inertial coordinate frame* defined by unit vectors **I**, **J**, and **K.** It is used for describing the motion of the elements.
2. *Local co-rotation frame* (**i**, **j**, **k**) defined in such a way that rigid-body motion of the element is eliminated. The origin is set at node 1 of the element and x-axis is drawn through node 2. Other two axes are defined in a suitable way.
3. *Section frames* (**l**, **m**, **n**), where vector **l** is normal to the cross-section of the element while vectors **m** and **n** are directed along principal directions of the cross sections. Element cross-sections rotate, but remain planar during the motion.

The co-rotational frame plays a fundamental role. It is a local frame whose orientation is defined by the matrix (**i j k**). Rotation of an element cross-section is defined by rotation matrix (**l m n**). A vector described by its coordinates in global frame is denoted by boldface, e.g. **e**, **f**. The same vector described by coordinates in the local frame is denoted by superscript 'e', e.g. $\mathbf{e}^e$, $\mathbf{f}^e$.

Detailed development of the bond graph beam finite element component is given in (Damic and Cohodar 2005). The component denoted by **Beam3D** has two power ports corresponding to two nodes of the beam element. It is developed using hierarchical multilevel component models. Thus, despite the rather complex mathematical relations that it involves, this approach enables their clear graphical representation. This component is used as the building block for developing flexible link models.

Processes at power ports are described by pairs of power vectors – efforts and flows. These are defined by linear and angular velocities and corresponding forces and moments at the element nodes

$$\mathbf{f}_i^T = \left(\mathbf{v}_i^T \quad \boldsymbol{\omega}_i^T\right),\ \mathbf{e}_i^T = \left(\mathbf{F}_i^T \quad \mathbf{T}_i^T\right)(i = 1,2). \tag{1}$$

An advantage of the co-rotational formulation is that it allows separation of element local deformations and large rigid body motions. This way, the effort at i-th element node can be represented as a sum of efforts corresponding to rigid body motion $\mathbf{e}_{ir}$ and local deformation $\mathbf{e}_{id}$:

$$\mathbf{e}_i = \mathbf{e}_{ir} + \mathbf{e}_{id} \quad (i = 1,2). \tag{2}$$

The system level model of the component is shown in Fig. 2. Branching of efforts described by Eq. (2) is represented by the left and the right **e** components, which are built of 1-junctions.

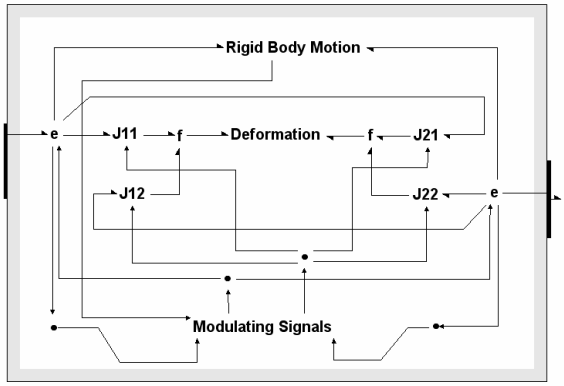

Figure 2: Bond graph model of 3D beam finite element

Local flows corresponding to deformation of the element with respect to the co-rotational frame can be represented as

$$\overline{\mathbf{f}}_1^e = \overline{\boldsymbol{\omega}}_1^e,\ \overline{\mathbf{f}}_2^{eT} = \left(\overline{v}_{2x}^e \quad \overline{\boldsymbol{\omega}}_2^{eT}\right). \tag{3}$$

Owing to the way in which the co-rotational frame is defined only rotation takes place at the left-end section, whereas, the right-end section, in addition to the rotation also undertakes displacement along local x-axis.

Transformations from the global to the local flows are described by relations

$$\bar{\mathbf{f}}_i^e = \mathbf{J}_{i1}\mathbf{f}_1^e + \mathbf{J}_{i2}\mathbf{f}_2^e \ (i=1,2)\,, \tag{4}$$

where $\mathbf{J}_{ij}$ (ij =1,2) are Jacobian matrices defined by

$$\mathbf{J}_{11} = \left(\begin{array}{ccc|ccc} 0 & 0 & -\eta/l & 0 & \eta & 0 \\ 0 & 0 & -1/l & 0 & 1 & 0 \\ 0 & 1/l & 0 & 0 & 0 & 1 \end{array}\right), \tag{5a}$$

$$\mathbf{J}_{12} = \left(\begin{array}{ccc|ccc} 0 & 0 & \eta/l & 0 & 0 & 0 \\ 0 & 0 & 1/l & 0 & 0 & 0 \\ 0 & -1/l & 0 & 0 & 0 & 0 \end{array}\right), \tag{5b}$$

$$\mathbf{J}_{21} = \left(\begin{array}{ccc|ccc} -1 & 0 & 0 & 0 & 0 & 0 \\ \hline 0 & 0 & -\eta/l & -1 & \eta & 0 \\ 0 & 0 & -1/l & 0 & 0 & 0 \\ 0 & 1/l & 0 & 0 & 0 & 0 \end{array}\right), \tag{5c}$$

$$\mathbf{J}_{22} = \left(\begin{array}{ccc|ccc} 1 & 0 & 0 & 0 & 0 & 0 \\ \hline 0 & 0 & \eta/l & 1 & 0 & 0 \\ 0 & 0 & 1/l & 0 & 1 & 0 \\ 0 & -1/l & 0 & 0 & 0 & 1 \end{array}\right). \tag{5d}$$

Here η is the ratio of x- and y- components of unit vector $\mathbf{m}_1$ of the left cross-section and l is the actual beam element length. These matrices correspond to the projector matrix of (Pacoste and Eriksson 1997) stripped of zero rows.

Transformations given by Eqs. (4) and (5) are represented in Fig. 2 by components **J11** to **J22** built of modulated transformers and two **f** components consisting of 0-junctions. The signals for modulation are generated by the component **Modulating Signals**.

2.2. Deformation of Beam Elements

To describe local deformation of the beam element, flows defined as time derivatives of local displacements of the end cross-sections are introduced:

$$\hat{\mathbf{f}}_1^e = \dot{\bar{\boldsymbol{\theta}}}_1^e, \quad \hat{\mathbf{f}}_2^{eT} = \left(\dot{\bar{u}}_2^e \quad \dot{\bar{\boldsymbol{\theta}}}_2^{eT}\right). \tag{6}$$

The corresponding efforts are given by

$$\hat{\mathbf{e}}_1^e = \left(\hat{T}_{1x}^e \quad \hat{T}_{1y}^e \quad \hat{T}_{1z}^e\right), \quad \hat{\mathbf{e}}_2^e = \left(\hat{F}_{2x}^e \quad \hat{T}_{2x}^e \quad \hat{T}_{2y}^e \quad \hat{T}_{2z}^e\right). \tag{7}$$

Finite rotation of the cross-sections are described using notation of rotation vector (Nour-Omid and Rankin 1991, Rankin and Brogan 1986). This way we find the following relationship between the flows:

$$\begin{pmatrix} \dot{\bar{\boldsymbol{\theta}}}_1^e \\ \dot{\bar{u}}_2^e \\ \dot{\bar{\boldsymbol{\theta}}}_2^e \end{pmatrix} = \begin{pmatrix} \boldsymbol{\Lambda}\left(\bar{\boldsymbol{\theta}}_1^e\right) & 0 & \mathbf{0} \\ \mathbf{0} & 1 & \mathbf{0} \\ \mathbf{0} & 0 & \boldsymbol{\Lambda}\left(\bar{\boldsymbol{\theta}}_2^e\right) \end{pmatrix} \begin{pmatrix} \bar{\boldsymbol{\omega}}_1^e \\ \bar{v}_{2x}^2 \\ \bar{\boldsymbol{\omega}}_2^e \end{pmatrix}. \tag{8}$$

Here

$$\boldsymbol{\Lambda}\left(\bar{\boldsymbol{\theta}}_i^e\right) = \mathbf{I} - \frac{1}{2}\tilde{\boldsymbol{\Theta}}_i^e + \frac{1}{4}\lambda\left(\theta/2\right)\left(\tilde{\boldsymbol{\Theta}}_i^e\right)^2 \ (i=1,2), \tag{9}$$

where $\tilde{\boldsymbol{\Theta}}_i^e$ is a skew-symmetric matrix corresponding to the rotation vector $\bar{\boldsymbol{\theta}}_i^e$ of the end cross-sections. Function λ is defined by

$$\lambda(\bullet) = \frac{1}{\bullet^2}\left(1 - \frac{\bullet}{\tan(\bullet)}\right). \tag{10}$$

Deformation of the element in the local frame is represented by component **Deformation** (Fig. 2), whose model is shown in Fig.3. The model follows Eqs. (8) to (10). The multiport capacitive component **C** describes the deformation of the element.

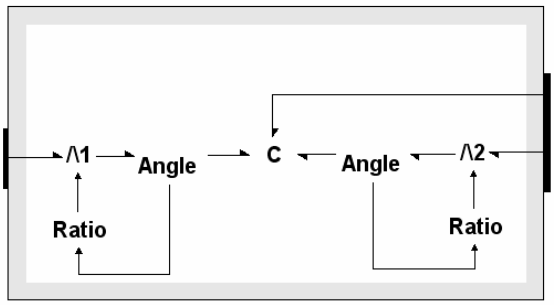

Figure 3: Model component **Deformation**

In this study Euler-Bernoulli's model of the beam is used. The end strains are defined, respectively, by

$$\bar{\varepsilon}_{2x}^e = \frac{\partial \bar{u}_2^e}{\partial x}, \qquad \bar{\kappa}_{ix}^e = \frac{\partial \bar{\theta}_{ix}^e}{\partial x}, \quad \bar{\kappa}_{iy}^e = \frac{\partial \bar{\theta}_{iy}^e}{\partial x}, \quad \bar{\kappa}_{iz}^e = \frac{\partial \bar{\theta}_{iz}^e}{\partial x} \ (i=1,2). \tag{11}$$

The strain energy reads (Pacoste and Eriksson 1997):

$$\begin{aligned} V = {} & \frac{EA}{2l_0}\left(\bar{u}_2^e\right)^2 + \frac{GI_t}{2l_0}\left(\bar{\theta}_{2x}^e - \bar{\theta}_{1x}^e\right)^2 + \\ & + \frac{2EI_y}{l_0}\left(\left(\bar{\theta}_{1y}^e\right)^2 + \left(\bar{\theta}_{2y}^e\right)^2 + \bar{\theta}_{1y}^e\bar{\theta}_{2y}^e\right) + \\ & + \frac{2EI_z}{l_0}\left(\left(\bar{\theta}_{1z}^e\right)^2 + \left(\bar{\theta}_{2z}^e\right)^2 + \bar{\theta}_{1z}^e\bar{\theta}_{2z}^e\right), \end{aligned} \tag{12}$$

where EA, GI_t, EI_y and EI_z are corresponding stiffnesses. The constitutive relation of the element is found by partial differentiation of the strain energy:

$$\hat{\mathbf{e}}_1^e = \frac{\partial V}{\partial \bar{\boldsymbol{\theta}}_1^e}, \quad \hat{\mathbf{e}}_2^e = \begin{pmatrix} \dfrac{\partial V}{\partial \bar{u}_2^e} \\ \dfrac{\partial V}{\partial \bar{\boldsymbol{\theta}}_2^e} \end{pmatrix}, \ (i,j=1,2). \tag{13}$$

Owing to the applied object-oriented approach and co-rotational formulation, the other deformation theories could be implemented as well, e.g. following Timoshenko's model. This could be achieved simply by

changing the constitutive relations of the capacitive component **C**.

2.3. Dynamics of Element Rigid Body Motion

Dynamics of overall motion of the element in the global frame is represented by component **Rigid Body Motion** at the top of Fig. 2. The corresponding model is developed using the quasy-continuous approach of (Avelo et al 1991) as described in (Damic and Cohodar 2005) and as shown in Fig. 4.

The coordinates used for describing the motion of the element are position vectors $\mathbf{r}_i$ of the origin of the end section frames and the triads of the section frames unit vectors. Corresponding flows are defined as

$$\mathbf{f}_{il} = \begin{pmatrix} \dot{\mathbf{r}}_i \\ \dot{\mathbf{m}}_i \\ \dot{\mathbf{n}}_i \end{pmatrix}, (i = 1,2). \tag{14}$$

The relationship between time derivatives of the unit vectors and the corresponding angular velocities of the end section frames is given by

$$\begin{aligned} \dot{\mathbf{m}}_i &= \tilde{\boldsymbol{\omega}}_i \mathbf{m}_i = -\tilde{\mathbf{m}}_i \boldsymbol{\omega}_i \\ \dot{\mathbf{n}}_i &= \tilde{\boldsymbol{\omega}}_i \mathbf{n}_i = -\tilde{\mathbf{n}}_i \boldsymbol{\omega}_i \end{aligned} \quad (i = 1,2), \tag{15}$$

where $\tilde{\bullet}$ denotes a skew-symmetric matrix corresponding to vector $\bullet$. These transformations are represented in Fig. 4 by components **Rot-m**, **Rot-n**, **mi** and **ni**.

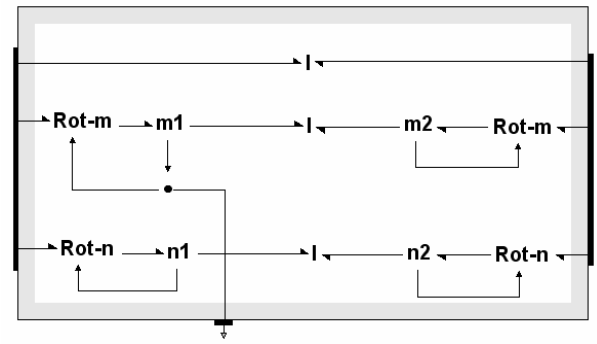

Figure 4: Model component **Rigid Body Motion**

Following the approach of (Avelo et al 1991) kinetic energy of the element can be written as

$$T = \frac{1}{2} \sum_{i=1}^{2} \sum_{j=1}^{2} \mathbf{f}_{il}^T \mathbf{M}_{ij} \mathbf{f}_{jl} \quad (i = 1,2), \tag{16}$$

where $\mathbf{M}_{ij}$ are constant mass matrices defined by

$$\mathbf{M}_{ij} = \begin{bmatrix} \rho c_{ij} A \mathbf{I}_3 & \mathbf{0} & \mathbf{0} \\ \mathbf{0} & \rho c_{ij} I_z \mathbf{I}_3 & \mathbf{0} \\ \mathbf{0} & \mathbf{0} & \rho c_{ij} I_y \mathbf{I}_3 \end{bmatrix}, (i = 1,2). \tag{17}$$

Here ρ is the element mass density, A is the cross-section area, I_y and I_z are the section moments of inertia, and l_0 is the beam element length. The parameters c_{ij} depend on the interpolation used inside the element.

Generalized momenta at the ports of inertial elements **I** (Fig. 4) are found by partial differentiation of the element kinetic energy with respect to corresponding flows:

$$\mathbf{p}_{il} = \mathbf{M}_{i1} \mathbf{f}_{1l} + \mathbf{M}_{i2} \mathbf{f}_{2l}, \quad (i = 1,2). \tag{18}$$

2.4. Modeling flexible links

Flexible links can be discretized in a certain number of beam finite elements, represented by **Beam3D** components. This can be achieved in different ways. The approach used here is to create first a kind of a *super element* component defined by five beam finite elements (Fig. 5). This component can be generated easily by copying **Beam3D** components from the library into the document using the *Copy* and *Paste* technique, and linking them into the document. These operations, however, are not simple copy and insertion operations, but really involve copying of the complete model trees (Damic and Montgomery 2003).

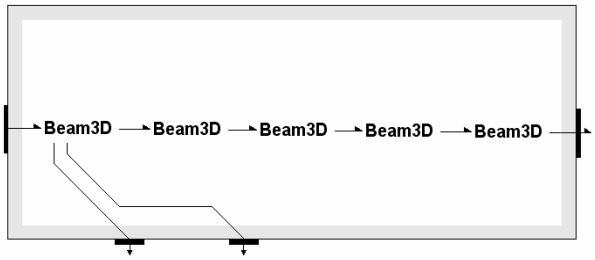

Figure 5: Model of a super element component

These components can be subsequently used to generate higher level components. This way, using the object-oriented approach, a flexible link can be easily decomposed in to a large number of finite elements. In this study the flexible links are modelled using two super elements connected port to port, and thus the links are descretized in a total of ten **Beam3D** components.

3. BOND GRAPH MODEL OF A JOINT

Let *i-th* revolute joint connect *i*-1st and *i-th* flexible links. Angular velocity of the first cross-section of the *i-th* link $\boldsymbol{\omega}_i$ is related to the angular velocity of the last cross-section of *i*-1st links $\boldsymbol{\omega}_{i-1}$ and to the angular velocity of *i-th* joint $\boldsymbol{\omega}_{i-1,i}$ by

$$\boldsymbol{\omega}_i = \boldsymbol{\omega}_{i-1} + \boldsymbol{\omega}_{i-1,i}. \tag{19}$$

It is assumed that the revolute joints are rigidly attached to the former link and that the mass and elasticity of the joint are neglected as well. To simplify things further, it is assumed that the joint axis coincides with one of the unit vectors of the right end cross-section frame. For example, if the joint axis coincides with unit vector $\mathbf{n}_2$,

as shown in Fig. 6, the joint angular velocity can be written as

$$\boldsymbol{\omega}_{i-1,i} = \dot{\theta}_i \cdot \mathbf{n}_2 , \qquad (20)$$

where $\dot{\theta}_i$ is the time derivative of the joint angle rotation.

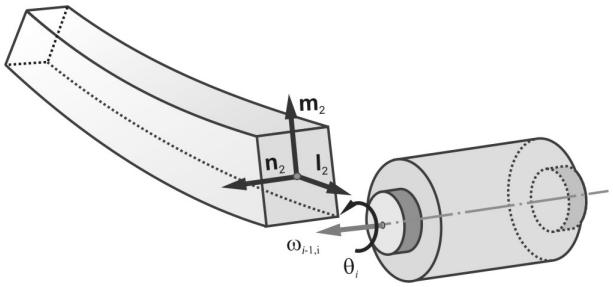

Figure 6: Typical joint orientation

The bond graph model of a revolute joint, which connects two flexible links, is shown in Fig. 7a. It consists of two components - **Revolute** (Fig. 7b) and **Drive** (Fig. 7d).

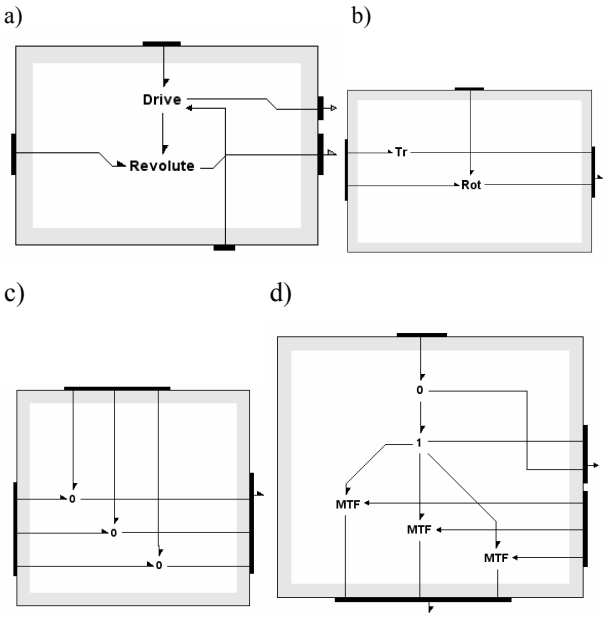

Figure 7: a) Revolute joint model, b) **Revolute**, c) **Rot** d) **Drive**

The **Revolute** component itself consists of two components. The **Tr** component represents the translation part of the joint model and consists of three 1-junctions for the translation in the directions of three axes. Component **Rot** consists of 0-junctions (Fig. 7c) and represents the relationship between the angular velocities given by Eq. (19). **Drive** consists of transformers **MTF** modulated by components of unit vector $\mathbf{n}_2$ in the global frame.

4. EXAMPLES

Two problems have been investigated. The first one treats a flexible planar double link using 3D models. It is chosen to test the approach developed and to compare it with the results reported in (Liu and Hong, 2003). A robot with an anthropomorphic arm has been chosen as the second example. It provides testing of the full three-dimensional behaviour of a multi-link manipulator under computer control.

Case 1: Flexible Double Links

Simulation of flexible two links planar arm, shown in Fig.8, is carried out to verify the developed model and to compare the simulation results with the published ones. Geometric properties and material data of the links are given in Table 1 (Liu and Hong 2003).

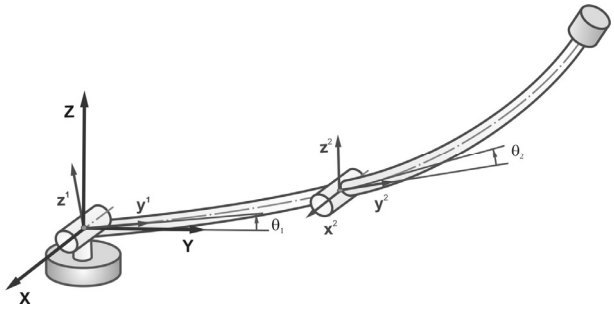

Figure 8: Flexible two links planar arm

Table 1: Properties of the flexible two links planar arm

Parameter	Values	
	Inner link	Outer link
Length [m]	8	8
Cross-section area [m^2]	3,84e-4	7,3e-5
Area moment inertia [m^4]	1,5e-7	8,218e-9
Young modulus [Pa]	6,8952e10	6,8952e10
Mass density [kg/m^3]	2,7667e3	2,7667e3

The prescribed motions of both links are as given in (Liu and Hong 2003). Rotation of the inner link is done from $\pi/2$ to 0 rad in 10 s. The rotation angle of the inner link is given by

$$\theta_1(t) = \begin{cases} \theta_0 - \left(\dfrac{\theta_0 - \theta_s}{T_s}\right)\left[t - \left(\dfrac{T_s}{2\pi}\right)\left(\sin\dfrac{2\pi t}{T_s}\right)\right], & 0 \le t \le T_s \\ \theta_s, & t > T_s \end{cases}, \qquad (21)$$

where $\theta_0 = \pi/2$, θ_s=0 and T_s = 10 s. The spin-up motion of the outer link is described by

$$\theta_2(t) = \begin{cases} \dfrac{\omega_s}{T_s}\left[\dfrac{t^2}{2} + \left(\dfrac{T_2}{2\pi}\right)^2\left(\cos\dfrac{2\pi t}{T_s} - 1\right)\right], & 0 \le t \le T_s \\ \omega_s\left(t - \dfrac{T_s}{2}\right), & t > T_s \end{cases}, \qquad (22)$$

where ω_s = 1 rad/s, T_s = 10 s.

Both links are modelled as flexible beams. The bond graph model of the arm is shown in Fig.9. The links are represented by components **Link 1** and **Link 2,** and are discretized in ten 3D finite elements each. The simulation has been run using the time step of 0.001 s and absolute and relative error tolerances of 1e-8.

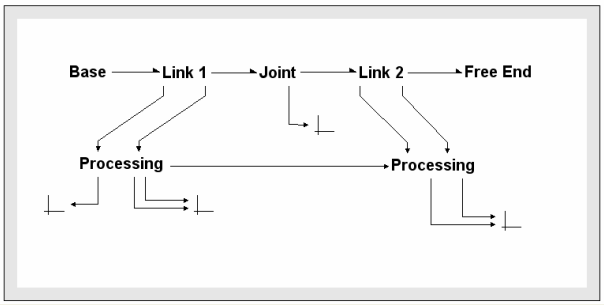

Figure 9: The project system level – Flexible two links

The results of simulations of the tip deflections of the inner and the outer links are shown in Fig. 10. The obtained results are in excellent agreement with the results reported in (Liu and Hong 2003).

a)

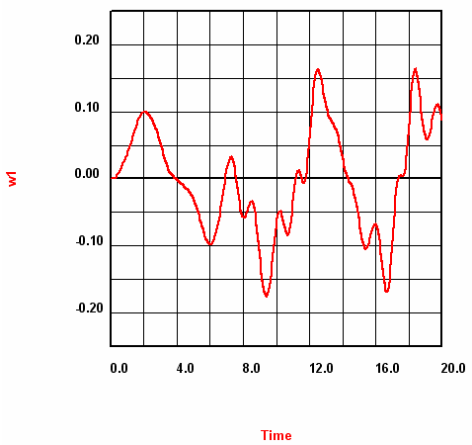

b)

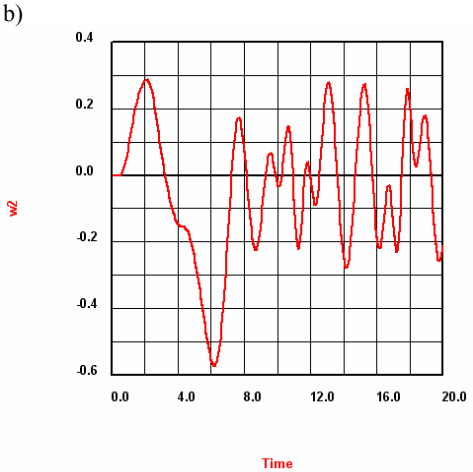

Figure 10: Simulation results: a) Inner link, b) Outer link

Case 2: Anthropomorphic Arm under Feedback Control

An anthropomorphic arm under closed-loop control is taken as the second example (Fig.11). The material and geometry parameters of the arm are given in Table 2 (Wehage at al. 1992).

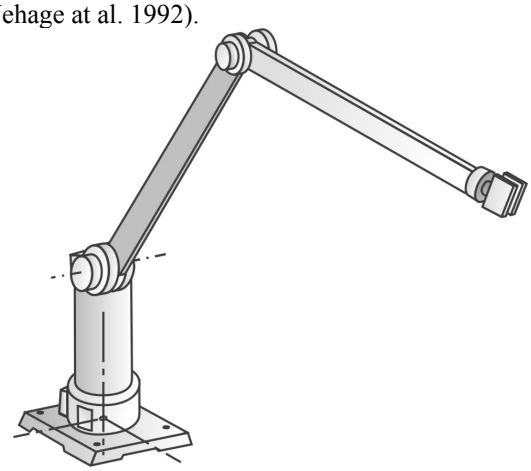

Figure 11: Sketch of the anthropomorphic arm

Table 2: Properties of the anthropomorphic arm

Parameter		Links		
		1	2	3
Length [m]		0,3	0,5	0,5
Cross-section area [mxm]		r=0,15	0,10x0,05	0,10x0,05
Mass [kg]		24,88	6,60	3,25
Mass mom. inertia [kgm^2]	*Ixx*	2,488e-1	6,875e-3	3,385e-3
	Iyy	1,244e-1	1,389e-1	6,839e-2
	Izz	2,488e-1	1,430e-1	7,042e-2
Young modulus [Pa]		0,699e11	0,699e11	1,727e11
Mass density [kg/m^3]		0,264e4	0,264e4	0,130e4

The manipulator is composed of three links with revolute joints and is driven by a controller that implements PD joint space control law. The trajectory in the operational space imposed on the end-effector is given by

$$X = 0,7 - 0,05\cos(2\pi t),$$
$$Y = 0,25t^2, \qquad (23)$$
$$Z = 0,05 + 0,25\sqrt{3} - 0,05\sin(2\pi t).$$

The system level model of the robot is given in Fig. 12a. It shows the main components that constitute the robot system: **Controller**, **Manipulator**, **Base** and **End**. Component **Base** defines that the robot base is fixed to the ground. Similarly **End** defines free effort conditions at the end-effector. The model of the anthropomorphic arm represented in Fig. 11 is given in Fig. 12b.

Two different models are analyzed: the manipulator with rigid (RL) and with flexible links (FL). For both cases the models at the first two levels look the same. Differences lie deeper, e.g. at levels of models of the links. Due to the way how models are defined, it is relatively easy to change between rigid-body and flexible-body models.

a)

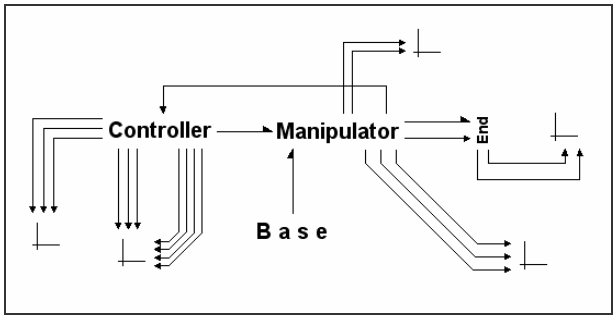

b)

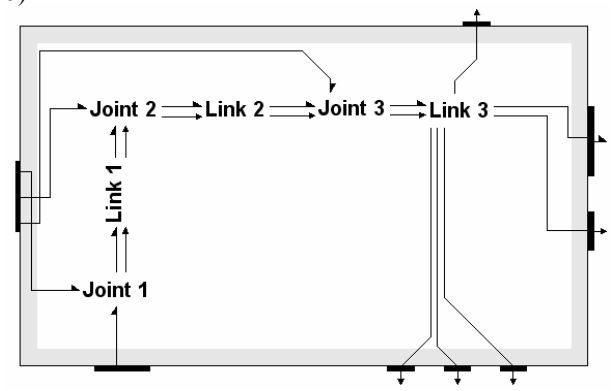

Figure 12: Model of the robot: a) System level model, b) Model of **Manipulator**

Bond Graph models of rigid multibody systems have been explained elsewhere (Damic and Montgomery 2003). In the flexible body model, the first link is assumed to be rigid, while the second and third are flexible. The flexible links are disretized by ten finite elements each, as explained in Sect. 2.4.

The controller part of this system is modelled by component **Controller**. **Manipulator** and **Controller** are joined by (multidimensional) power bond line that is used to control the revolute joints actuators. Likewise, control signals from the joints angular velocity and position sensors are fed back to the controller. More details are given in (Cohodar 2005).

In order to compare simulation results, the same values of proportional and derivative gains are taken in both simulations, i.e. K_P = 1000, K_D = 1000 for all axes. The simulations were undertaken for 1 s, with output interval of 0.001 s. The standard absolute and relative error tolerances of 1e-6 were used. The results are shown in Fig. 13a-f.

Figures 13a and 13b show the joint torques for the flexible-body and rigid-body models. Position errors of the end-effector in the joint space are depicted in Figs. 13c and 13d. They are of order of the magnitude of 1e-4 m in both models. Elastic deformations for flexible-body models of the third and the second link are very small – of order of magnitude of 1e-7 m for the third link, and 1e-6 m for the second link as shown in Figs. 13e and 13f.

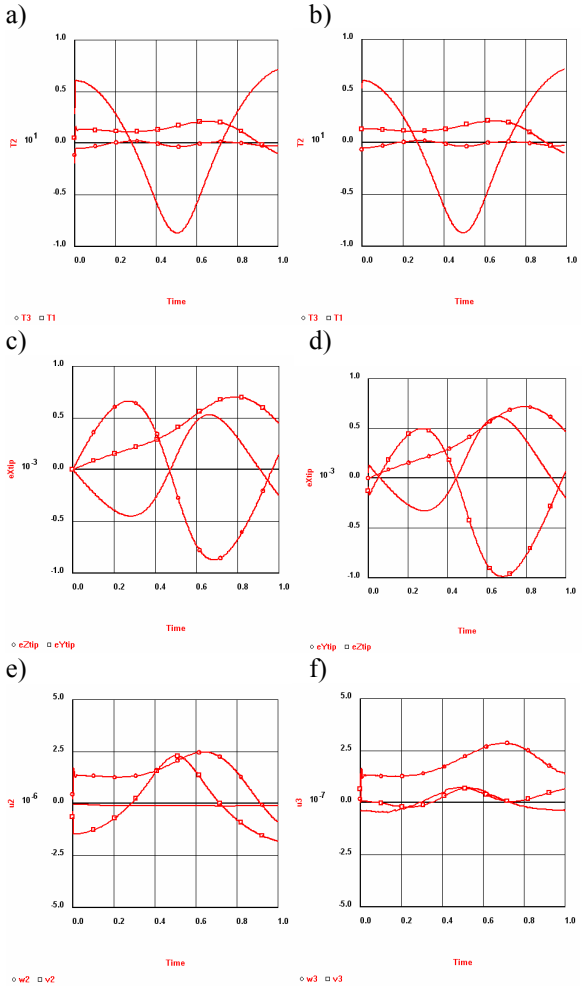

Figure 13: Simulation results: a) Joint torques (FL), b) Joint torques (RL), c) Errors in end-effector position (FL), d) Errors in end-effector position (RL), e) Elastic deformation of the third link, f) Elastic deformation of the second link

Comparison of simulation results for the flexible-body and rigid-body models demonstrates effectiveness of joint space PD control in flexible-body simulation. Better accuracy could be obtained using higher values of gains, but in that case oscillations could arise.

CONCLUSION

The paper presents the bond graph approach to modelling and simulation of flexible multibody systems. The approach is characterized by a combination of systematic top-down model decomposition and model build-up using library components. To deal with

flexible multibody systems, finite element modelling is used based on bond graph 3D beam components.

The finite element component model is based on co-rotational formulation, which offers nonlinear framework for modelling flexible multibody systems. It can be used for systematic development of dynamical models in essentially the same way as when treating systems as rigid. This was illustrated on two examples. Comparison of the simulation results with data reported in literature shows excellent agreement and demonstrates that the method developed can be effectively used to solve complex control problems in robotics.

Modelling and simulations described in the paper were developed in an object-oriented modelling and simulation environment - *BondSim*. It was specifically designed to deal with complex modelling and simulations tasks.

REFERENCES

Avelo, A.; J. Garcia de Jalon; and E. Bayo. 1991. "Dynamics of flexible multibody systems using Cartesian co-ordinates and large displacement theory". Int. J. for Num. Methods in Engineering, 32:1543-1563.

Cohodar, M. 2005. "Modelling and simulation of robot system with flexible links using bond graphs", PhD Thesis. University of Sarajevo, (july).

Crisfield, M.A. and G.F. Moita, 1996. "A Unified Co-rotational Framework for Solids, Shells and Beams". Int. J. Solids Structures, 33:2969-2992.

Damic, V. 2006. (to appear). "Modelling flexible body systems: a bond graph component model approach". Mathematical and Computer Modelling of Dynamical Systems, 12:175-187.

Damić, V. and M. Čohodar. 2005. "A Bond Graph Approach to Modeling of Spatial Flexible Multibody Systems Based on Co-rotational Formulation". ICBGM'05 (New Orleans, Lousiana Jan.23-27), 37: 213-218.

Damić, V. and J. Montgomery. 2003. *Mechatronics by Bond Graphs: An Object-Oriented Approach to Modelling*. Springer-Verlag, Berlin-Heidelberg.

Favre, W. and S. Scavarda. 1998."Bond Graph Representation of Multibody Systems with Kinematic Loops". Journal of the Franklin Institute, 335B, 643-660.

Liu, J. and J. Hong. 2003. "Geometrical stiffening of flexible link with large overall motion". *Computers & Structures*. 81, 1113-1124.

Karnopp, D. 1997. "Understanding Multibody Dynamics Using Bond Graph Representations". Journal of the Franklin Institute, 334B, 4, 631-642.

Margolis, D.J. and D. Karnopp 1979. "Bond Graphs for Flexible Multibody Systems". Trans. ASME, J. Dynamic Systems, Measurement and Control, 101(1): 50-57.

Nour-Omid, B. and C.C. Rankin. 1991. "Finite Rotations Analysis and Consistent Linearization Using Projector". Computer Methods in Applied Mechanics and Engineering, 93, 361-384.

Pacoste, C. and A. Eriksson. 1997. "Beam Elements in Instability problems". Int. J. for Numerical Methods in Engineering, 144, 163-197.

Rankin, C.C. and F.A. Brogan. 1986. "An Element Independent Corotational Procedure for the Treatment of Large Rotations". ASME Journal of Pressure Vessel Technology, 108, 165-174.

Shabana, A.A. 1998. Dynamics of Multibody Systems, 2nd Edn. *Cambridge University Press*, Cambridge.

Wehage, R.A.; A.A. Shabana; and Y.L. Hwang. 1992. "Projection Methods in Flexible Multibody Dynamics. Part II: Dynamics and Recursive Projection Methods". Int. J. Numer. Meth. Engng., 43, 1941-1966.

AUTHOR BIOGRAPHIES

VJEKOSLAV DAMIC was born in Sarajevo, Bosnia and Herzegovina. He studied Mechanical Engineering at University of Sarajevo, where he also received his PhD degree in 1985. The title of the thesis was "Systematic study of transient processes in electro-hydraulic servo-systems". In the thesis, dynamic behaviour of high-performance electro-hydraulic servos was studied using bond graphs. One of the results of the thesis was a bond graph modelling and simulation program written in FORTRAN (for WAX 750 computers). He worked in the Research Institute for Automatic Control for over 20 years. In 1992 he moved to the University of Dubrovnik, Croatia, where he is teaching Engineering Mechanics, Object-oriented programming, and Computer Simulations. He is engaged in research on bond graph modelling and simulation in mechatronics. In particular he is interested in differential-algebraic systems methods in bond graphs setting, computational algebra and modern object-oriented developments. In 2003 he published jointly with Dr. John Montgomery a book on bond graph modelling in Mechatronics and developed program *BondSim*. His e-mail address is: vdamic@unidu.hr.

MAJDA COHODAR graduated from the Faculty of Mechanical Engineering, University of Sarajevo and obtained her degree in 1990. She received her M.Sc. degree in Mechanical Engineering from the University of Zagreb, Faculty of Mechanical Engineering and Naval Architecture, in 1999 and her PhD in 2005 from the University of Sarajevo. The title of her PhD thesis was "Modelling and simulation of a robot system with flexible links using bond graphs". In her scientific work, she has been occupied with modelling of mechatronics systems using the bond graph technique. Her e-mail address is: cohodar@mef.unsa.ba.